International Journal of Solids and Structures 48 (2011) 2349–2360

Contents lists available at ScienceDirect

International Journal of Solids and Structures

journal homepage: www.elsevier.com/locate/ijsolstr

Strain-based geometrically nonlinear beam formulation for modeling very flexible aircraft

Weihua Su *, Carlos E.S. Cesnik

Department of Aerospace Engineering, University of Michigan, Ann Arbor, MI 48109-2140, USA

ARTICLE INFO

Article history:
Received 26 November 2010
Received in revised form 20 January 2011
Available online 24 April 2011

Keywords:
Geometrically nonlinear beam
Strain-based formulation
Structural dynamics
Very flexible aircraft

ABSTRACT

This paper introduces a strain-based geometrically nonlinear beam formulation for structural and aeroelastic modeling and analysis of slender wings of very flexible aircraft. With beam extensional strain, twist, and bending curvatures defined as the independent degrees of freedom, the equations of motion are derived through energy methods. Some special treatments are applied to the formulation to effectively model split-beam systems and beam configurations with multiple nodal displacement constraints. Using the strain-based formulation, solutions of different beam configurations under static loads and forced dynamic excitations are compared against ones from other geometrically nonlinear beam formulations.

© 2011 Elsevier Ltd. All rights reserved.

1. Introduction

In structural dynamic and aeroelastic analysis of very flexible aircraft (e.g., glider and high-altitude long-endurance aircraft), the slender wings of these aircraft can be modeled as beams by taking advantage of the structure slenderness. However, the high flexibility associated with the wings brings some special requirements to the beam formulation applied to the analysis. From the previous investigations (Patil et al., 2000, 2001a,b), the slender wings of very flexible aircraft may undergo large deformations under normal operating loads, exhibiting geometrically nonlinear behaviors. The aeroelastic behavior of the aircraft may change significantly due to the large deflection of the flexible wings. In addition, very flexible aircraft usually see the coupling between the low-frequency elastic modes of their slender wings and the rigid-body motion of the complete aircraft (Livne and Weisshaar, 2003; Patil et al., 2001b; Shearer and Cesnik, 2007; Su and Cesnik, 2010). Therefore, the coupled effects between the large deflection due to the wing flexibility and the aeroelastic/flight dynamic characteristics of the complete aircraft must be properly accounted for in a nonlinear aeroelastic solution. For this purpose, a beam formulation that is able to capture the geometrically nonlinear wing deformation is required to serve as the basis of the nonlinear aeroelastic analysis of very flexible aircraft. Moreover, in the modeling of aircraft structures, the complete aircraft is represented by a multiple-connected flexible beam system. Such beam system may feature split and joint between beam members, resulting in a statically indeterminate structure. An example of such layout is the joined-wing sensorcraft configuration (Tilmann et al., 2003).

There have been different geometrically nonlinear formulations established for slender beams. One may classify them based on the solution methodology, namely the displacement-based formulation, the mixed-form formulation, and the strain (or stress)-based formulation. Their difference lies in the definition of independent variables to represent the displacement field and the treatment of the beam reference line's rotation in the solution. Palacios and Cesnik (2009) comprehensively discussed the three types of beam formulations for the structural, aeroelastic, and flight dynamic analysis of very flexible aircraft. They compared the solutions in terms of their numerical efficiency and simplicity for integrated flight dynamic analysis with full aircraft flexibility.

A common approach to solve the geometrically nonlinear beam is to use a displacement-based formulation. An implementation of this type of formulation can be found in Bauchau and Hong (1988), where displacements and rotations of the beam reference line were defined as the irreducible set of solution variables. The main advantages of this formulation are: (1) displacement constraints can be easily applied, and (2) numerical solution algorithms are abundant and well addressed in the literature. However, the complexity of this formulation and its corresponding order of the nonlinearities are high. These result in high computational cost for the solution.

To solve the geometrically nonlinear beams in a more computationally effective way, one of the alternatives is the mixed-form geometrically exact formulation, e.g., Hodges (1990). Lagrange multipliers are used to satisfy the equations of motion with constitutive and kinematics relations in the formulation. The mixed-form

* Corresponding author. Tel.: +1 734 936 0541.
E-mail addresses: suw@umich.edu (W. Su), cesnik@umich.edu (C.E.S. Cesnik).

0020-7683/$ - see front matter © 2011 Elsevier Ltd. All rights reserved.
doi:10.1016/j.ijsolstr.2011.04.012

Nomenclature

$\overline{A}$	coefficient matrix in solving member kinematics
$A(s)$	beam cross-sectional area
B	body reference frame
B^F, B^M	influence matrices for the distributed forces and moments
b	local auxiliary reference frame defined at each node along beam reference line
D_{nm}	direction cosines that accounts for the beam reference line slope discontinuities from element m to element n
D^{bw}	direction cosines between the local w frame and the b frame at the same node
F_a	inertia force at an arbitrary point a
F^{dist}, F^{pt}	distributed and point forces
f	any internal or external load applied to the beam
G	global (inertial) reference frame
$\mathbb{G}(s)$	$\mathbb{K}(s)(s-s_0)$, matrix of strain components for the solution of beam kinematics
g	gravity acceleration column vector
h	absolute positions and orientations of beam nodes, represented by the w frame base vectors
$\bar{h}$	column vector consisting of the unknown nodal positions and orientations
h^*	column vector consisting of the boundary condition in solving member kinematics
h^b	absolute positions and orientations of beam nodes, represented by the b frame base vectors
I	identity matrix
I_{ij}	mass moment of inertia of the beam cross section about its shear center ($i,j = x,y,z$)
J	Jacobian matrix
$\mathbb{K}(s)$	matrix of strain components
K_c	total generalized stiffness matrix due to additional displacement constraints
K_{ca}, K_{cr}	generalized stiffness matrices for absolute and relative displacement constraints, respectively
$k(s)$, $c(s)$	beam cross-sectional stiffness and structural damping matrices
$M^{cs}(s)$	beam cross-sectional inertia matrix
M, C, K	discrete mass, damping, and stiffness matrices of the whole system
M_e, C_e, K_e	element mass, damping, and stiffness matrices
M_F, C_F, K_F	generalized mass, damping, and stiffness matrices of the whole system
M^{dist}, M^{pt}	distributed and point moments
m	mass per unit length, kg/m
N	influence matrix for the gravity force
p, p_w	position of the w frame with respect to the B frame
p_a	position of an arbitrary point a with respect to the G frame
p_b	position of the b frame with respect to the B frame
R	generalized load vector
R_c	total generalized load vector due to additional displacement constraints
R_{ca}, R_{cr}	generalized load vector for absolute and relative displacement constraints, respectively
r_x, r_y, r_z	position of the cross-sectional mass center in the w frame
s	beam curvilinear coordinate, m
s_0	curvilinear coordinate of the root of a beam member, m
u	corresponding displacement due to any internal or external load f applied to the beam
V	volume of the beam
W_a	virtual work at an arbitrary point a
W^{ext}, W^{int}	external and internal virtual work, respectively
w	local beam reference frame defined at each node along beam reference line
x, y, z	position of an arbitrary point a in the corresponding local w frame, m
α	stiffness-proportional damping coefficient
α_N	numerical damping in geometrically nonlinear static solutions
ε	elastic strain vector
ε_e	element elastic strain vector, including extension, twist, out-of-plane, and in-plane bending
ε^0	initial (prescribed) elastic strain vector
θ	rotations of beam nodes, rad
λ_c	total Lagrange multipliers vector
λ_{ca}, λ_{cr}	Lagrange multipliers for absolute and relative displacement constraints, respectively
Π	energy functional of the system
Π^*	modified energy functional with displacement constraints introduced
ρ	beam material density, kg/m^3

Subscripts

e	element
$h\varepsilon$	h vector with respect to the strain ε
$p\varepsilon$	nodal position with respect to the strain ε
x, y, z	directions of base vectors of a reference frame
$\theta\varepsilon$	nodal rotation with respect to the strain ε

formulation has its advantages over the displacement-based formulation, which include relaxation of the continuity of the shape functions and possible higher solution accuracy (Zienkiewicz and Taylor, 2000). The formulation allows for a simple solution scheme (Hodges et al., 1996) and has been applied to the analysis of rotor blades (Shang et al., 1999) and a complete very flexible aircraft (Patil et al., 2000, 2001b). Another application of the mixed-form formulation can be found in the work of Palacios and Cesnik (2008), where a numerical framework was developed using this formulation to model slender beams with embedded piezoelectric materials. The low-order formulation can provide high accuracy for the modeling, design, and analysis of slender structures. In the mixed-form formulation presented by Hodges (1990), the beam rotations were still solved as independent degrees of freedom. An updated mixed-form solution was introduced in Hodges (2003), where nodal velocities and beam curvatures were defined as the structural states of the beam. This formulation avoids the direct solution of the beam rotations, which can reduce the computational cost in the solution. However, it brings difficulties in modeling the statically indeterminate beams. Overall, the mixed-form formulation is suitable for the nonlinear aeroelastic and flight dynamic problems of very flexible aircraft, which feature low-frequency responses and large wing motions.

The strain-based approach is another effective solution to the geometrically nonlinear beam problems. Examples of this type of beam formulation can be found in the literature (Gams et al., 2007a,b; Planinc et al., 2001; Zupan and Saje, 2003). Common in these beam solutions, strains and curvatures of the beam reference line are primary variables to represent the beam deformation. Since no direct integration of beam rotations is required, the strain-based formulation allows for simple shape functions (Gams et al., 2007a). The shear locking phenomena is also avoided in strain-based solutions (Ryu and Sin, 1996; Zupan and Saje, 2003). In addition, the internal forces and moments can be easily

determined in these solutions from the strain variables without differentiation operations that are usually required in displacement-based solutions. The accuracy of the internal forces and moments is of the same order as the accuracy of the independent variables (Zupan and Saje, 2003). The strain-based beam equations can be solved with a simple time-integration scheme (Gams et al., 2007a), and has been applied to the geometrically nonlinear problems of curved beams and other slender structures.

This paper presents a strain-based approach to address the nonlinear aeroelastic and control problems of very flexible aircraft. The proposed formulation defines the extensional strain, bending and twist curvatures of the beam reference line as the independent degrees of freedom, while transverse shears are not explicitly included in them. Unlike the strain-based formulations presented in the literature (e.g., Zupan and Saje, 2003), which enforce the beam equilibrium equation and strain–displacement kinematics simultaneously with Lagrange multipliers, the proposed strain-based formulation solves these equations iteratively. Thus, the derived governing equation is the classic form of second-order differential equation, which simplifies the solution process. For that, the force and displacement boundary conditions are considered in a new way and the modeling of multiple-connected beam systems is addressed by using Lagrange multiplier. These improvements in this new formulation make it more flexible in modeling arbitrary beam configurations under different loading conditions. Besides the above-mentioned advantages, the strain-based formulation brings additional benefits to control studies, since the curvatures are the variables that can be directly measured by the strain sensors. This formulation may also demonstrate great computational efficiency, due to the reduction in degrees of freedom for the same complex deformation when compared to the displacement-based or the mixed-form formulations. Lastly, the strain-based formulation is efficient in solving geometrically nonlinear static problems, as it features a constant stiffness matrix (for statically determinate beams). This advantage, however, does not hold in nonlinear transient solutions, where the inertia and damping of the system need to be updated according to the instantaneous beam deformation states. While the authors and co-workers have used aspects of this beam formulation for aeroelastic problems (Cesnik and Brown, 2002; Shearer and Cesnik, 2007; Su and Cesnik, 2010), this paper presents the complete treatment of the strain-based geometrically nonlinear beam formulation. The finite-element equations of motion are derived with the modeling capability of multiple-connected and statically indeterminate beams. Numerical studies highlighting the features and modeling capabilities of the strain-based beam formulation are also presented.

2. Theoretical formulation

In this formulation, the nonlinear beam is allowed fully coupled three-dimensional extensional, twisting, and bending deformations. The equations of motion for the beam are derived by applying the principle of virtual work and the variation of energy functional.

2.1. System frames

As shown in Fig. 1(a), a fixed global (inertial) frame G is firstly defined. A body frame $B(t)$ is then built in the global frame to describe the vehicle position and orientation, with $B_x(t)$ pointing to the right wing, $B_y(t)$ pointing forward, and $B_z(t)$ being cross product of $B_x(t)$ and $B_y(t)$.

Within the body frame, a local beam frame w is built at each node along the beam reference line (Fig. 1(b)), which is used to define the nodal position and orientation. Vectors $w_x(s,t)$, $w_y(s,t)$, and

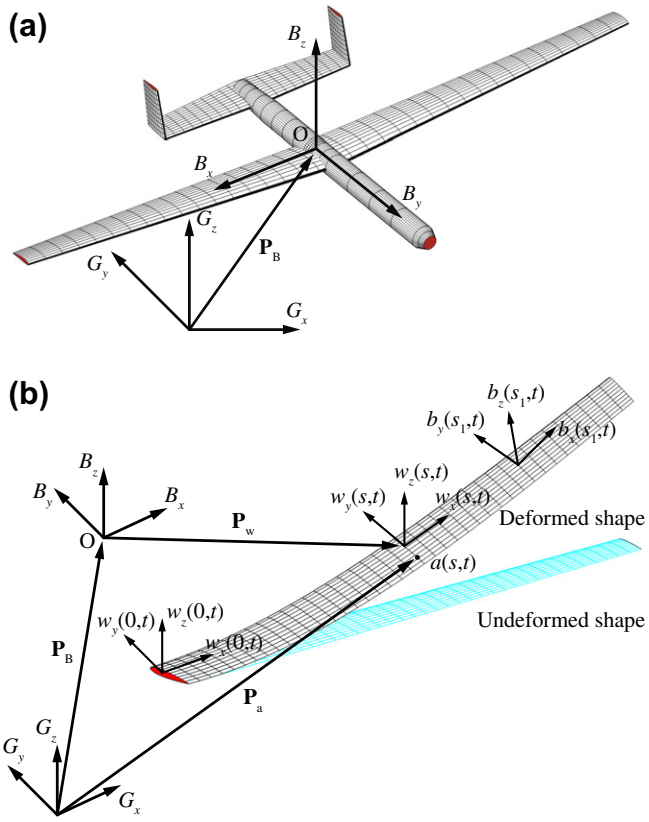

Fig. 1. Basic beam reference frames: (a) global and body frame defining the rigid-body motion of aircraft; (b) flexible lifting-surface frames within body frame.

$w_z(s,t)$ are bases of the beam frame, whose directions are pointing along the beam reference axis, toward the leading edge (front), and normal to the beam surface, respectively, resolved in the body frame. s is the curvilinear beam coordinate.

To facilitate the modeling process, another auxiliary reference frame $b(s,t)$ is also defined at each node. This frame is aligned with the body frame B upon the beam initialization. However, it may undergo both translations and rotations due to the beam deformation and the rigid-body motion of the vehicle. The b frame is useful for modeling the relative nodal displacement constraints that will be discussed in Section 2.7. Note that the w frame and the b frame will be aligned if there is no sweeping, dihedral, and pre-twist of the beam at its initial configuration.

2.2. Fundamental descriptions of elements

A nonlinear beam element is developed to model the elastic deformation of slender beams. Strain degrees (curvatures) of the beam reference line are considered as the independent variables in the solution. The strain-based formulation allows simple shape functions for the strain degrees in the element. Constant-value functions are used here. Thus, the strain vector of an element is denoted as

$$\varepsilon_e = \{\, \varepsilon_x \quad \kappa_x \quad \kappa_y \quad \kappa_z \,\}^T \tag{1}$$

where ε_x is the extensional strain, κ_x, κ_y, and κ_z are the twist of the beam reference line, bending about the local w_y axis, and bending about the local w_z axis, respectively. The total strain vector of the complete aircraft is obtained by stacking the element strain vectors:

$$\varepsilon^T = \{\, \varepsilon_{e1}^T, \quad \varepsilon_{e2}^T, \quad \varepsilon_{e3}^T, \quad \dots \,\} \tag{2}$$

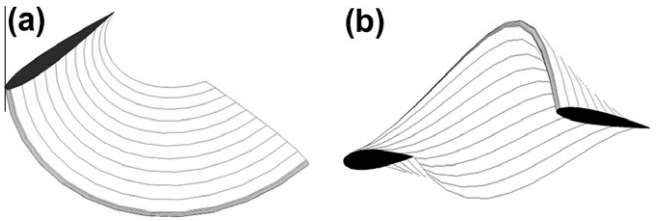

Fig. 2. Deformations of a constant-strain element: (a) circular shape; (b) spiral shape.

Transverse shear strains are not explicitly included in this equation. However, shear strain effects are included in the constitutive relation (Cesnik and Hodges, 1997). Complex geometrically nonlinear deformations can be represented by such a constant strain distribution over each element. For example, a single element can be deformed into a circle or a spiral (Fig. 2). To represent the quadratic nodal displacement field that will be recovered from the constant strain, the element is defined with three equally spaced nodes. Some of the functions, such as inertia and distributed load, are assumed to vary linearly between the three nodes of each element. The values of these functions over the element can be obtained from its nodal values using linear Lagrange interpolation functions.

The position and orientation of each node are defined by a vector consisting of 12 components, denoted as

$$h(s)^T = \{\, p_w(s)^T, \quad w_x(s)^T, \quad w_y(s)^T, \quad w_z(s)^T \,\} \tag{3}$$

where p_w is the position of the w frame resolved in the body frame. The governing equations to be derived will solve for the curvatures (strains) of the beam reference line directly. The nodal position and rotation h are dependent variables, which will be recovered from the curvatures through the kinematic relations. Details about the kinematics will be discussed in Section 2.5. For the convenience of deriving the equations of motion, nodal rotations θ, about the local beam reference frame, are also used as interim variables in this formulation. They are eventually eliminated from the governing equations through the strain-rotation relations (Section 2.5).

2.3. Internal virtual work

The equations of motion of the system are derived by following the principle of virtual work. The total virtual work done on a beam is found by integrating the products of all internal and external forces and the corresponding virtual displacements over the volume, which is given as

$$\delta W = \int_V \delta u^T(x,y,z) f(x,y,z) dV \tag{4}$$

where f represents general forces acting on a differential volume. This may include internal elastic forces, inertial forces, gravity forces, external distributed forces and moments, external point forces and moments, etc. δu is the corresponding virtual displacement. When beam cross-sectional properties are known, the integration of Eq. (4) over the beam volume is simplified to the integration along the beam coordinate s. This integration is first numerically performed over each beam element, followed by the assemblage of the element quantities to obtain the total virtual work on the whole beam.

2.3.1. Internal virtual work due to inertias

With the B frame and the G frame (Fig. 1) coincident, the position and acceleration of an arbitrary point a, in the beam is given as

$$\begin{aligned} p_a &= p_w + x w_x + y w_y + z w_z \\ \ddot{p}_a &= \ddot{p}_w + x \ddot{w}_x + y \ddot{w}_y + z \ddot{w}_z \end{aligned} \tag{5}$$

where (x,y,z) is the position of point a within the local beam frame w. The virtual work done on a differential volume due to the inertial force is given by

$$\delta W_a = \delta p_a^T dF_a \tag{6}$$

with

$$\begin{aligned} \delta p_a &= \delta p_w + x \delta w_x + y \delta w_y + z \delta w_z \\ dF_a &= -\ddot{p}_a(\rho dA(s) ds) \\ &= -(\ddot{p}_w + x \ddot{w}_x + y \ddot{w}_y + z \ddot{w}_z)(\rho dA(s) ds) \end{aligned} \tag{7}$$

where ρ is the material density. Substituting Eq. (7) into Eq. (6) yields

$$\begin{aligned} \delta W_a = &-\left(\delta p_w^T + x \delta w_x^T + y \delta w_y^T + z \delta w_z^T\right) \\ &\left(\ddot{p}_w + x \ddot{w}_x + y \ddot{w}_y + z \ddot{w}_z\right) \rho dA(s) ds \end{aligned} \tag{8}$$

The virtual work done by the inertia force along the beam coordinate s can be obtained by integrating Eq. (8) over each cross section, leading to

$$\delta W^{int}(s) = -\delta h^T(s) M(s) \ddot{h}(s) \tag{9}$$

where

$$\begin{aligned} M^{cs}(s) &= \int_{A(s)} \rho \begin{bmatrix} 1 & x & y & z \\ x & x^2 & xy & xz \\ y & yx & y^2 & yz \\ z & zx & zy & z^2 \end{bmatrix}_{12\times 12} dA \\ &= \begin{bmatrix} m & mr_x & mr_y & mr_z \\ mr_x & \frac{1}{2}(I_{yy}+I_{zz}-I_{xx}) & I_{xy} & I_{xz} \\ mr_y & I_{yx} & \frac{1}{2}(I_{zz}+I_{xx}-I_{yy}) & I_{yz} \\ mr_z & I_{zx} & I_{zy} & \frac{1}{2}(I_{xx}+I_{yy}-I_{zz}) \end{bmatrix}_{12\times 12} \end{aligned} \tag{10}$$

$M^{cs}(s)$ is the cross-sectional inertial matrix, with each entry being a 3 by 3 diagonal matrix, $A(s)$ is the cross-sectional area, m is the mass per unit span at each cross section, (r_x, r_y, r_z) is the position of the cross-sectional mass center in the w frame, and I_{ij} are the cross-sectional mass moments of inertia about the reference axis.

2.3.2. Internal virtual work due to strains and strain rates

The virtual work due to the internal strains is

$$\delta W^{int}(s) = -\delta\varepsilon(s)^T k(s)(\varepsilon(s) - \varepsilon^0(s)) \tag{11}$$

where $\varepsilon^0(s)$ is the initial strain upon the beam initialization, $k(s)$ is the cross-sectional stiffness matrix. The entries of $k(s)$ come from an appropriate beam cross-sectional solution (Cesnik and Hodges, 1997; Palacios and Cesnik, 2005).

Internal damping is added to the formulation to better model the actual behavior of the structure. A stiffness-proportional damping is used in the current formulation, given by

$$c(s) = \alpha k(s) \tag{12}$$

where α is the stiffness-proportional damping coefficient. Thus, the virtual work due to the strain rates is

$$\delta W^{int}(s) = -\delta\varepsilon^T(s) c(s) \dot{\varepsilon}(s) \tag{13}$$

2.3.3. Internal virtual work on element

To obtain the total internal virtual work on each element, one needs to summate Eqs. (9), (11), and (13), and then to integrate

the summation over the length of the element. In practice, the integration is performed numerically, given as

$$\delta W_e^{int} = -\delta h_e^T M_e \ddot{h}_e - \delta \varepsilon_e^T C_e \dot{\varepsilon}_e - \delta \varepsilon_e^T K_e (\varepsilon_e - \varepsilon_e^0) \tag{14}$$

where

$$\begin{aligned} K_e &= k\Delta s \\ C_e &= c\Delta s \\ M_e &= \tfrac{1}{2}\Delta s \begin{bmatrix} \frac{1}{4}M_1^{cs} + \frac{1}{12}M_2^{cs} & \frac{1}{12}M_1^{cs} + \frac{1}{12}M_2^{cs} & 0 \\ \frac{1}{12}M_1^{cs} + \frac{1}{12}M_2^{cs} & \frac{1}{12}M_1^{cs} + \frac{1}{2}M_2^{cs} + \frac{1}{12}M_3^{cs} & \frac{1}{12}M_2^{cs} + \frac{1}{12}M_3^{cs} \\ 0 & \frac{1}{12}M_2^{cs} + \frac{1}{12}M_3^{cs} & \frac{1}{12}M_2^{cs} + \frac{1}{4}M_3^{cs} \end{bmatrix} \end{aligned} \tag{15}$$

ε_e in Eq. (14) is the element strain, Δs is the initial element length, K_e is the element stiffness matrix, C_e is the element damping matrix, M_e is the element inertia matrix, and M_i^{cs} are the cross-sectional inertia matrices at each node of an element.

2.4. External virtual work

2.4.1. Gravitational virtual work

The virtual work of gravity force on a differential volume can be obtained by following the similar approach to the virtual work of the inertial force, given by

$$\delta W_a = -\left(\delta p_w^T + x\delta w_x^T + y\delta w_y^T + z\delta w_z^T\right)\rho g dA(s) ds \tag{16}$$

where g is the gravity acceleration column vector. The virtual work on a differential beam cross section due to the gravity force is found by integration of Eq. (16) over each cross section, yielding

$$\delta W^{ext}(s) = -\delta h^T(s) N(s) g ds \tag{17}$$

where $N(s)$ is related with the inertia properties of the cross section:

$$N(s) = \int_{A(s)} \rho \begin{bmatrix} 1 \\ x \\ y \\ z \end{bmatrix}_{12\times 3} dA \tag{18}$$

The total virtual work due to the gravity force on each element is found by integrating Eq. (17) over the element length, resulting in

$$\delta W_e^{ext} = -\delta h_e^T N_e g \tag{19}$$

where

$$N_e = \frac{1}{2}\Delta s \begin{bmatrix} \frac{1}{3}N_1 + \frac{1}{6}N_2 \\ \frac{1}{6}N_1 + \frac{2}{3}N_2 + \frac{1}{6}N_3 \\ \frac{1}{6}N_2 + \frac{1}{3}N_3 \end{bmatrix}_{36\times 3} \tag{20}$$

with N_i being the inertia property $N(s)$ evaluated at each node of an element.

2.4.2. Virtual work due to distributed forces

With the assumption that distributed forces on each element and their corresponding virtual displacements vary linearly between the nodes of the element, the element virtual work due to distributed forces is obtained as

$$\delta W_e^{ext} = \int_{\Delta s} \delta p^T(s) F^{dist}(s) ds = \delta p_e^T B_e^F F_e^{dist} \tag{21}$$

where

$$\delta p_e = \begin{Bmatrix} \delta p_1 \\ \delta p_2 \\ \delta p_3 \end{Bmatrix}_{9\times 1}, \quad B_e^F = \frac{1}{2}\Delta s \begin{bmatrix} \frac{1}{3} & \frac{1}{6} & 0 \\ \frac{1}{6} & \frac{2}{3} & \frac{1}{6} \\ 0 & \frac{1}{6} & \frac{1}{3} \end{bmatrix}_{9\times 9}, \quad F_e^{dist} = \begin{Bmatrix} F_1^{dist} \\ F_2^{dist} \\ F_3^{dist} \end{Bmatrix}_{9\times 1} \tag{22}$$

δp_i and F_i^{dist} are the virtual displacement and force per unit length at node i, respectively. Note that the variable p in the above equations refers to p_w, with the subscript w omitted for simplicity. Each entry of B_e^F is a 3 by 3 diagonal matrix.

2.4.3. Virtual work due to distributed moments

The virtual work due to distributed moments is obtained in a similar way to that of the distributed forces

$$\delta W_e^{ext} = \int_{\Delta s} \delta\theta^T(s) M^{dist}(s) ds = \delta\theta_e^T B_e^M M_e^{dist} \tag{23}$$

where

$$\delta\theta_e = \begin{Bmatrix} \delta\theta_1 \\ \delta\theta_2 \\ \delta\theta_3 \end{Bmatrix}_{9\times 1}, \quad B_e^M = \frac{1}{2}\Delta s \begin{bmatrix} \frac{1}{3} & \frac{1}{6} & 0 \\ \frac{1}{6} & \frac{2}{3} & \frac{1}{6} \\ 0 & \frac{1}{6} & \frac{1}{3} \end{bmatrix}_{9\times 9}, \quad M_e^{dist} = \begin{Bmatrix} M_1^{dist} \\ M_2^{dist} \\ M_3^{dist} \end{Bmatrix}_{9\times 1} \tag{24}$$

$\delta\theta_i$ and M_i^{dist} are the virtual displacement and force per unit length at node i, respectively. Each entry of B_e^M is also a 3 by 3 diagonal matrix.

2.4.4. Virtual work due to point forces

The virtual work on an element due to external point forces is obtained by the following summation:

$$\delta W_e^{ext} = \sum_{i=1}^{3} \delta p_i^T F_i^{pt} = \delta p_e^T F_e^{pt} \tag{25}$$

where

$$F_e^{pt} = \begin{Bmatrix} F_1^{pt} \\ F_2^{pt} \\ F_3^{pt} \end{Bmatrix}_{9\times 1} \tag{26}$$

with F_i^{pt} being the point force at node i.

2.4.5. Virtual work due to point moments

The virtual work on an element due to point moments is obtained in a similar way to that of the point forces, i.e.,

$$\delta W_e^{ext} = \sum_{i=1}^{3} \delta\theta_i^T M_i^{pt} = \delta\theta_e^T M_e^{pt} \tag{27}$$

where

$$M_e^{pt} = \begin{Bmatrix} M_1^{pt} \\ M_2^{pt} \\ M_3^{pt} \end{Bmatrix}_{9\times 1} \tag{28}$$

with M_i^{pt} being the point moment at node i.

2.5. Kinematics

The kinematics is solved for each member (for single-beam systems, Fig. 3(a)) or each group of members (for split-beam systems, Fig. 3(b)). A member is defined as an assemblage of elements, which may include beam reference line slope discontinuities, variation in the discretization level, and change of cross-sectional properties. A set of members that originate from one common root member forms one group. The root of each member is either

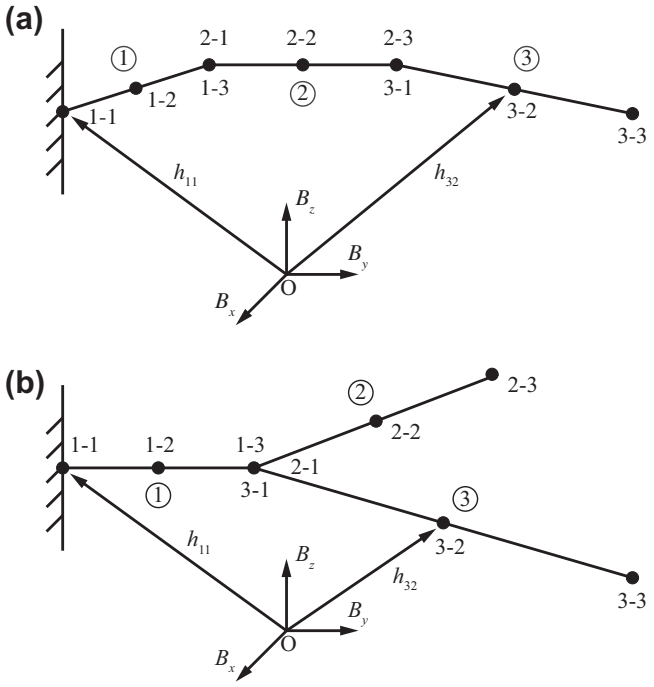

Fig. 3. Sketches of single-beam and split-beam systems: (a) single-beam system (one member consisting of three elements); (b) split-beam system (one group formed by three members, each member consisting of one element).

prescribed or solved from the tip of its "parent" member. The nodal positions and orientations within a member are obtained by marching the kinematics from its root node to the end node of the last element.

The equation that relates the dependent displacements to the independent strains is given by Cesnik and Brown (2003)

$$\frac{\partial h(s)}{\partial s} = \mathbb{K}(s)h(s) \tag{29}$$

with $\mathbb{K}(s)$ being a matrix function of the strains, i.e.,

$$\mathbb{K}(s) = \begin{bmatrix} 0 & 1+\varepsilon_x(s) & 0 & 0 \\ 0 & 0 & \kappa_z(s) & -\kappa_y(s) \\ 0 & -\kappa_z(s) & 0 & \kappa_x(s) \\ 0 & \kappa_y(s) & -\kappa_x(s) & 0 \end{bmatrix} \tag{30}$$

Note that each entry in the above matrix is a 3 by 3 diagonal matrix. With the assumption that each element has a constant strain state, the solution of Eq. (29) is given by

$$h(s) = e^{\mathbb{K}\cdot(s-s_0)}h_0 = e^{\mathbb{G}(s)}h_0 \tag{31}$$

where h_0 is the displacement of a fixed or prescribed root node of the beam (boundary condition). For a three-node element, the solution can be performed by using the discrete form:

$$\begin{aligned} h_{n1} &= D_{nm}h_{m3} \\ h_{n2} &= e^{\frac{1}{2}\mathbb{K}_n\Delta s}h_{n1} = e^{\mathbb{G}_n}h_{n1} \\ h_{n3} &= e^{\frac{1}{2}\mathbb{K}_n\Delta s}h_{n2} = e^{\mathbb{G}_n}h_{n2} \end{aligned} \tag{32}$$

where element n is the current element with the length of Δs, and element m is the one to which element n is attached. h_{ni} is the displacement of the ith node of element n. D_{nm} is the rotation matrix with direction cosines that accounts for the slope discontinuities of the beam reference lines from element m to element n. The solutions for kinematics for single-beam and split-beam systems are different due to the different connection relations.

2.5.1. Single-beam system

For a single-beam system shown in Fig. 3(a), kinematics for a member is obtained by marching the element kinematics from the boundary node to the end node. Following Eq. (32), the marching procedure can be written as:

$$\begin{aligned} &h_{11} = h_0 \quad h_{21} = D_{21}h_{13} \quad h_{31} = D_{32}h_{23} \\ &h_{12} = e^{\mathbb{G}_1}h_{11} \quad h_{22} = e^{\mathbb{G}_2}h_{21} \quad h_{32} = e^{\mathbb{G}_3}h_{31} \\ &h_{13} = e^{\mathbb{G}_1}h_{12} \quad h_{23} = e^{\mathbb{G}_2}h_{22} \quad h_{33} = e^{\mathbb{G}_3}h_{32} \end{aligned} \tag{33}$$

These equations can be arranged in matrix form as

$$\begin{bmatrix} I & & & & & & & & & \\ -e^{\mathbb{G}_1} & I & & & & & & & & \\ & -e^{\mathbb{G}_1} & I & & & & & & & \\ & & -D_{21} & I & & & & & & \\ & & & -e^{\mathbb{G}_2} & I & & & & & \\ & & & & -e^{\mathbb{G}_2} & I & & & & \\ & & & & & -D_{32} & I & & & \\ & & & & & & -e^{\mathbb{G}_3} & I & & \\ & & & & & & & -e^{\mathbb{G}_3} & I \end{bmatrix} \begin{Bmatrix} h_{11} \\ h_{12} \\ h_{13} \\ h_{21} \\ h_{22} \\ h_{23} \\ h_{31} \\ h_{32} \\ h_{33} \end{Bmatrix} = \begin{Bmatrix} h_0 \\ 0 \\ 0 \\ 0 \\ 0 \\ 0 \\ 0 \\ 0 \\ 0 \end{Bmatrix} \tag{34}$$

where the empty entries in the matrix correspond to zeros. Eq. (34) can be written into a compact form as

$$\bar{A}(\varepsilon)\bar{h}(\varepsilon) = h^* \tag{35}$$

where $\bar{h}$ is a column vector consisting of nodal positions and orientations of all nodes in the member, and h^* is a column vector consisting of the boundary condition. By solving Eq. (35), the dependent variables (displacements) of each node can be recovered from the independent variables (strains).

The Jacobian matrices reflecting the derivative of the displacements with respect to small changes in the strains are obtained by the differential of Eq. (35).

$$J_{h\varepsilon} = \frac{dh}{d\varepsilon} = -\bar{A}(\varepsilon)^{-1}\frac{d}{d\varepsilon}(\bar{A}(\varepsilon)\bar{h}(\varepsilon)) \tag{36}$$

Jacobian matrix of $J_{p\varepsilon}$, relating the nodal translations to small changes in the strains, is constructed by selecting the appropriate rows of $J_{h\varepsilon}$. This is intuitive as the nodal position p_w is a component of the nodal displacement h (see Eq. (3)). The relationship between an infinitesimal nodal rotation and an infinitesimal change in the unit direction vectors of local beam frame w is given by

$$d\theta = \begin{Bmatrix} d\theta_x \\ d\theta_y \\ d\theta_z \end{Bmatrix} = \begin{Bmatrix} w_z^T dw_y \\ w_x^T dw_z \\ w_y^T dw_x \end{Bmatrix} \tag{37}$$

Then the Jacobian matrix $J_{\theta\varepsilon}$ that relates the nodal rotations to small changes in the strains is found using subsets of $J_{h\varepsilon}$ and the current value of the unit direction vectors of the w frame, given by

$$J_{\theta\varepsilon} = \frac{d\theta}{d\varepsilon} = \begin{bmatrix} \frac{d\theta_x}{d\varepsilon} \\ \frac{d\theta_y}{d\varepsilon} \\ \frac{d\theta_z}{d\varepsilon} \end{bmatrix} = \begin{bmatrix} w_z^T \frac{dw_y}{d\varepsilon} \\ w_x^T \frac{dw_z}{d\varepsilon} \\ w_y^T \frac{dw_x}{d\varepsilon} \end{bmatrix} \tag{38}$$

where $dw_x/d\varepsilon$, $dw_y/d\varepsilon$, and $dw_z/d\varepsilon$ are subsets of $J_{h\varepsilon}$. With the Jacobians defined, the variation and derivatives of the dependent vari-

able h, p, and θ are related to those of the independent strain variables as:

$$\begin{aligned} &\delta h = J_{h\varepsilon}\delta\varepsilon \quad dh = J_{h\varepsilon}d\varepsilon \\ &\delta p = J_{p\varepsilon}\delta\varepsilon \quad \dot{h} = J_{h\varepsilon}\dot{\varepsilon} \\ &\delta\theta = J_{\theta\varepsilon}\delta\varepsilon \quad \ddot{h} = J_{h\varepsilon}\ddot{\varepsilon} + \dot{J}_{h\varepsilon}\dot{\varepsilon} \end{aligned} \tag{39}$$

2.5.2. Split-beam system

Kinematics for members of a split-beam system (Fig. 3(b)) is still obtained by marching the element kinematics from the boundary node to each of the end nodes. However, the marching procedure is slightly different, because of the existence of the split point.

In the connections shown in Fig. 3(b), the first nodes of elements 2 and 3 are both connected with the last node of element 1. Therefore, h_{21} and h_{31} are both related with h_{13}, with different direction cosines, given by

$$\begin{aligned} &h_{11} = h_0 \quad h_{21} = D_{21}h_{13} \quad h_{31} = D_{31}h_{13} \\ &h_{12} = e^{\mathbb{G}_1}h_{11} \quad h_{22} = e^{\mathbb{G}_2}h_{21} \quad h_{32} = e^{\mathbb{G}_3}h_{31} \\ &h_{13} = e^{\mathbb{G}_1}h_{12} \quad h_{23} = e^{\mathbb{G}_2}h_{22} \quad h_{33} = e^{\mathbb{G}_3}h_{32} \end{aligned} \tag{40}$$

These can be written in matrix form as

$$\begin{bmatrix} I & & & & & & & & \\ -e^{\mathbb{G}_1} & I & & & & & & & \\ & -e^{\mathbb{G}_1} & I & & & & & & \\ & & -D_{21} & I & & & & & \\ & & & -e^{\mathbb{G}_2} & I & & & & \\ & & & & -e^{\mathbb{G}_2} & I & & & \\ & & -D_{31} & & & & I & & \\ & & & & & & -e^{\mathbb{G}_3} & I & \\ & & & & & & & -e^{\mathbb{G}_3} & I \end{bmatrix} \begin{Bmatrix} h_{11} \\ h_{12} \\ h_{13} \\ h_{21} \\ h_{22} \\ h_{23} \\ h_{31} \\ h_{32} \\ h_{33} \end{Bmatrix} = \begin{Bmatrix} h_0 \\ 0 \\ 0 \\ 0 \\ 0 \\ 0 \\ 0 \\ 0 \\ 0 \end{Bmatrix} \tag{41}$$

where again the empty entries in the matrix correspond to zeros. The solution of Eq. (41) yields the displacements of a split-beam system from strains. Note that the solution of Jacobian matrices for the split-beam system is obtained in the same way as the single-beam system.

2.6. System equations of motion

The total virtual work on the system is obtained by summing up all elements' internal and external work

$$\begin{aligned} \delta W &= \sum \left(\delta W_e^{int} + \delta W_e^{ext} \right) \\ &= -\delta h^T M\ddot{h} - \delta\varepsilon^T C\dot{\varepsilon} - \delta\varepsilon^T K(\varepsilon - \varepsilon^0) - \delta h^T Ng + \delta p^T B^F F^{dist} \\ &\quad + \delta\theta^T B^M M^{dist} + \delta p^T F^{pt} + \delta\theta^T M^{pt} \end{aligned} \tag{42}$$

After the assemblage of the global equations, the strain vector ε, the nodal displacement vector h, and all other variables and matrices for all flexible members have been appropriately sized, based on the beam discretization. The dependent variables can be replaced by the independent variable by applying the Jacobians (Eq. (39)). Therefore, the total virtual work on the whole beam can be written into the strain-based form as

$$\begin{aligned} \delta W &= -\delta\varepsilon^T J_{h\varepsilon}^T M(J_{h\varepsilon}\ddot{\varepsilon} + \dot{J}_{h\varepsilon}\dot{\varepsilon}) - \delta\varepsilon^T C\dot{\varepsilon} - \delta\varepsilon^T K(\varepsilon - \varepsilon^0) - \delta\varepsilon^T J_{h\varepsilon}^T Ng \\ &\quad + \delta\varepsilon^T J_{p\varepsilon}^T B^F F^{dist} + \delta\varepsilon^T J_{\theta\varepsilon}^T B^M M^{dist} + \delta\varepsilon^T J_{p\varepsilon}^T F^{pt} + \delta\varepsilon^T J_{\theta\varepsilon}^T M^{pt} \end{aligned} \tag{43}$$

The equations of motion can be obtained by letting the total virtual work be zero. Since the variation $\delta\varepsilon$ is arbitrary, the elastic system equations of motion are derived as

$$M_F(\varepsilon,t)\ddot{\varepsilon} + C_F(\varepsilon,\dot{\varepsilon},t)\dot{\varepsilon} + K_F\varepsilon = R(\varepsilon,t) \tag{44}$$

where

$$\begin{aligned} &M_F(\varepsilon,t) = J_{h\varepsilon}^T M J_{h\varepsilon} \quad C_F(\varepsilon,\dot{\varepsilon},t) = C + J_{h\varepsilon}^T M\dot{J}_{h\varepsilon} \quad K_F = K \\ &R(\varepsilon,t) = K_F\varepsilon^0 - J_{h\varepsilon}^T Ng + J_{p\varepsilon}^T B^F F^{dist} + J_{\theta\varepsilon}^T B^M M^{dist} + J_{p\varepsilon}^T F^{pt} + J_{\theta\varepsilon}^T M^{pt} \end{aligned} \tag{45}$$

One may note that the stiffness matrix K_F in Eq. (45) is constant and the geometrical nonlinearity is associated with the force vector R. This feature may simplify nonlinear static solutions.

2.7. Modeling additional nodal displacement constraints

From the solution of member kinematics, one can find the prescribed displacement at the member root is naturally imposed in the strain-based formulation. The additional displacement constraints are introduced using the Lagrange multiplier method. The derivation starts from the energy functional. Without loss of generality, consider a simplified form of the energy functional of a nonlinear beam in the current formulation, given by

$$\Pi = \frac{1}{2}\int_L k(s)\varepsilon^2 ds - R\varepsilon \tag{46}$$

where $k(s)$ is cross-sectional stiffness, L is the beam span, and R is the generalized load. The constraint formulation will be different, depending on the type of constraints.

2.7.1. Absolute displacement constraints

A cantilever beam is constrained at an arbitrary point (Fig. 4). The additional constraint can be introduced into the energy functional by applying a Lagrange multiplier:

$$\Pi^* = \frac{1}{2}\int_L k(s)\varepsilon^2 ds - R\varepsilon + \lambda_{ca}(h(l) - h^0(l)) \tag{47}$$

where λ_{ca} is the Lagrange multiplier, $h(l)$ is the displacement (position and/or rotations) of the constrained point, and $h^0(l)$ is the initial displacement of the constrained point. The variation of the functional is

$$\delta\Pi^* = \int_L k(s)\varepsilon\delta\varepsilon ds - R\delta\varepsilon + \lambda_{ca}\delta h(l) + \delta\lambda_{ca}(h(l) - h^0(l)) \tag{48}$$

The above equation can be discretized and written in matrix form, yielding

$$\delta\Pi^* = \delta\varepsilon^T K_F\varepsilon - \delta\varepsilon^T R + \delta\varepsilon^T J_{h\varepsilon}^T(l)\lambda_{ca} + \delta\lambda_{ca}^T(h(l) - h^0(l)) \tag{49}$$

where $J_{h\varepsilon}(l)$ is the Jacobian matrix evaluated at the constrained point.

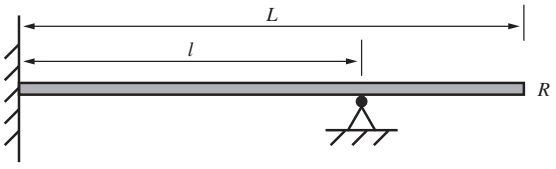

Fig. 4. Cantilever beam with absolute nodal displacement constraint.

The variation of the functional is zero, which yields the equilibrium equation of the system with the additional absolute displacement constraints. However, it is still necessary to handle the variable of $h(l)$, which is a function of the independent variable ε. The solution is performed in an iterative procedure. Assume the independent variable, ε, and the dependent variable $h(l)$, have been solved at step i, which are ε_i and $h_i(l)$, respectively. Then, the variation of the energy functional at step $i+1$ can be written as

$$\delta\varepsilon_{i+1}^T K_F \varepsilon_{i+1} + \delta\varepsilon_{i+1}^T (J_{h\varepsilon}(l))_i^T (\lambda_{ca})_{i+1} + \delta(\lambda_{ca})_{i+1}^T (h_{i+1}(l) - h^0(l)) = \delta\varepsilon_{i+1}^T R_i \tag{50}$$

The displacement can be written into the incremental form as

$$h_{i+1}(l) = h_i(l) + \delta h_{i+1}(l) = h_i(l) + (J_{h\varepsilon}(l))_i(\varepsilon_{i+1} - \varepsilon_i) \tag{51}$$

Substituting Eq. (51) into Eq. (50) yields

$$\begin{aligned}&\delta\varepsilon_{i+1}^T K_F \varepsilon_{i+1} + \delta\varepsilon_{i+1}^T (J_{h\varepsilon}(l))_i^T (\lambda_{ca})_{i+1} + \delta(\lambda_{ca})_{i+1}^T (J_{h\varepsilon}(l))_i \varepsilon_{i+1} \\ &\quad = \delta\varepsilon_{i+1}^T R_i + \delta(\lambda_{ca})_{i+1}^T (J_{h\varepsilon}(l))_i \varepsilon_i - \delta(\lambda_{ca})_{i+1}^T \left(h_i(l) - h^0(l)\right)\end{aligned} \tag{52}$$

which can be simplified to

$$\begin{aligned}&\left\{\delta\varepsilon_{i+1}^T \quad \delta(\lambda_{ca})_{i+1}^T\right\}\begin{bmatrix} K_F & (K_{ca})_i^T \\ (K_{ca})_i & 0\end{bmatrix}\begin{Bmatrix}\varepsilon_{i+1} \\ (\lambda_{ca})_{i+1}\end{Bmatrix} \\ &\quad = \left\{\delta\varepsilon_{i+1}^T \quad \delta(\lambda_{ca})_{i+1}^T\right\}\begin{Bmatrix} R_i \\ (R_{ca})_i\end{Bmatrix}\end{aligned} \tag{53}$$

where

$$\begin{aligned}(K_{ca})_i &= (J_{h\varepsilon}(l))_i \\ (R_{ca})_i &= (K_{ca})_i \varepsilon_i - \left(h_i(l) - h^0(l)\right)\end{aligned} \tag{54}$$

Therefore, the equilibrium equation of the system is given in a generalized form as

$$\begin{bmatrix} K_F & (K_{ca})_i^T \\ (K_{ca})_i & 0\end{bmatrix}\begin{Bmatrix}\varepsilon_{i+1} \\ (\lambda_{ca})_{i+1}\end{Bmatrix} = \begin{Bmatrix} R_i \\ (R_{ca})_i\end{Bmatrix} \tag{55}$$

Note that the Jacobian $(J_{h\varepsilon}(l))_i$ and its transpose are both updated at each solution step.

2.7.2. Relative displacement constraints

For the beam configurations with two members joining at a common point (Fig. 5), these members should be considered together and an inter-member displacement constraint should be imposed. Let the uth node of member m be coincident with the vth node of member n upon initialization. The positions and orientations of the two nodes are always constrained to be the same. In terms of position, this relation can be written simply as

$$h_{mu}^b = h_{nv}^b \tag{56}$$

where h^b is the position and orientation vector of the b frame with respect to the body frame B, whose definition is similar to h, except that the rotations are expressed using the b frame base vectors:

$$h^b \equiv \left\{p_b^T \quad b_x^T \quad b_y^T \quad b_z^T\right\}^T = \left\{p_w^T \quad b_x^T \quad b_y^T \quad b_z^T\right\}^T \tag{57}$$

Eq. (56) can be transformed into the local beam frame w by applying the individual rotation matrix

$$D_{mu}^{bw} h_{mu} - D_{nv}^{bw} h_{nv} = 0 \tag{58}$$

where D^{bw} contains the direction cosines between the nodal w frame and the b frame (Cesnik and Brown, 2003). h_{mu} and h_{nv} are the nodal displacement vectors expressed using the w frame base vectors (as defined in Eq. (3)).

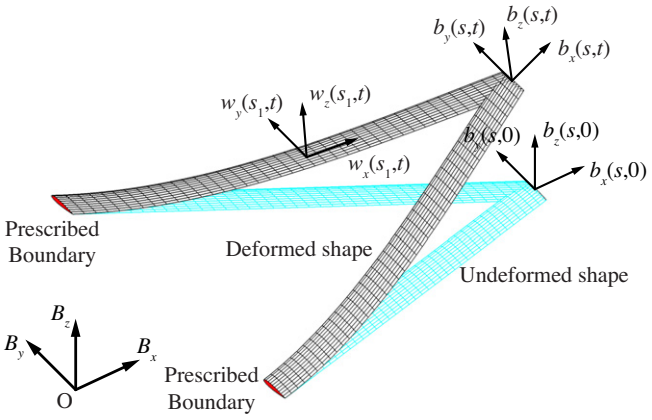

Fig. 5. Joined-beam configuration.

Therefore, the corresponding constrained energy functional and its variation are

$$\begin{aligned}\Pi^* &= \tfrac{1}{2}\int_L k(s)\varepsilon^2 ds - R\varepsilon + \lambda_{cr}\left(D_{mu}^{bw} h_{mu} - D_{nv}^{bw} h_{nv}\right) \\ \delta\Pi^* &= \int_L k(s)\varepsilon\delta\varepsilon ds - R\delta\varepsilon + \lambda_{cr}\delta\left(D_{mu}^{bw} h_{mu} - D_{nv}^{bw} h_{nv}\right) + \delta\lambda_{cr}\left(D_{mu}^{bw} h_{mu} - D_{nv}^{bw} h_{nv}\right)\end{aligned} \tag{59}$$

The discrete form of the variation can be given by

$$\begin{aligned}\delta\Pi^* = {}& \delta\varepsilon^T K_F \varepsilon - \delta\varepsilon^T R + \delta\varepsilon^T (J_{h\varepsilon}(mu))^T \left(D_{mu}^{bw}\right)^T \lambda_{cr} \\ & - \delta\varepsilon^T (J_{h\varepsilon}(nv))^T \left(D_{nv}^{bw}\right)^T \lambda_{cr} + \delta\lambda_{cr}^T D_{mu}^{bw} h_{mu} - \delta\lambda_{cr}^T D_{nv}^{bw} h_{nv}\end{aligned} \tag{60}$$

where $J_{h\varepsilon}(mu)$ and $J_{h\varepsilon}(nv)$ are the Jacobian matrices evaluated at the constrained nodes, respectively.

Following the same procedure as described in the previous section, the variation is written in the iterative form:

$$\begin{aligned}&\delta\varepsilon_{i+1}^T K_F \varepsilon_{i+1} + \delta\varepsilon_{i+1}^T \left[(J_{h\varepsilon}(mu))_i^T \left(D_{mu}^{bw}\right)^T - (J_{h\varepsilon}(nv))_i^T \left(D_{nv}^{bw}\right)^T\right](\lambda_{cr})_{i+1} \\ &\quad + \delta(\lambda_{cr})_{i+1}^T \left(D_{mu}^{bw}(h_{mu})_{i+1} - D_{nv}^{bw}(h_{nv})_{i+1}\right) = \delta\varepsilon_{i+1}^T R_i\end{aligned} \tag{61}$$

where

$$\begin{aligned}(h_{mu})_{i+1} &= (h_{mu})_i + \delta(h_{mu})_{i+1} = (h_{mu})_i + (J_{h\varepsilon}(mu))_i(\varepsilon_{i+1} - \varepsilon_i) \\ (h_{nv})_{i+1} &= (h_{nv})_i + \delta(h_{nv})_{i+1} = (h_{nv})_i + (J_{h\varepsilon}(nv))_i(\varepsilon_{i+1} - \varepsilon_i)\end{aligned} \tag{62}$$

Substituting Eq. (62) into Eq. (61) yields

$$\begin{aligned}&\delta\varepsilon_{i+1}^T K_F \varepsilon_{i+1} + \delta\varepsilon_{i+1}^T \left[(J_{h\varepsilon}(mu))_i^T \left(D_{mu}^{bw}\right)^T - (J_{h\varepsilon}(nv))_i^T \left(D_{nv}^{bw}\right)^T\right](\lambda_{cr})_{i+1} \\ &\quad + \delta(\lambda_{cr})_{i+1}^T \left[D_{mu}^{bw}(J_{h\varepsilon}(mu))_i - D_{nv}^{bw}(J_{h\varepsilon}(nv))_i\right]\varepsilon_{i+1} = \delta\varepsilon_{i+1}^T R_i \\ &\quad + \delta(\lambda_{cr})_{i+1}^T \left[D_{mu}^{bw}(J_{h\varepsilon}(mu))_i - D_{nv}^{bw}(J_{h\varepsilon}(nv))_i\right]\varepsilon_i - \delta(\lambda_{cr})_{i+1}^T \left(D_{mu}^{bw}(h_{mu})_i \right. \\ &\quad \left. - D_{nv}^{bw}(h_{nv})_i\right)\end{aligned} \tag{63}$$

which can be written into the matrix form as

$$\begin{aligned}&\left\{\delta\varepsilon_{i+1}^T \quad \delta(\lambda_{cr})_{i+1}^T\right\}\begin{bmatrix} K_F & (K_{cr})_i^T \\ (K_{cr})_i & 0\end{bmatrix}\begin{Bmatrix}\varepsilon_{i+1} \\ (\lambda_{cr})_{i+1}\end{Bmatrix} \\ &\quad = \left\{\delta\varepsilon_{i+1}^T \quad \delta(\lambda_{cr})_{i+1}^T\right\}\begin{Bmatrix} R_i \\ (R_{cr})_i\end{Bmatrix}\end{aligned} \tag{64}$$

where

$$(K_{cr})_i = D^{bw}_{mu}(J_{h\varepsilon}(mu))_i - D^{bw}_{n\nu}(J_{h\varepsilon}(n\nu))_i$$
$$(R_{cr})_i = (K_{cr})_i\varepsilon_i - \left(D^{bw}_{mu}(h_{mu})_i - D^{bw}_{n\nu}(h_{n\nu})_i\right) \tag{65}$$

Therefore, the equilibrium equation of the system is given by

$$\begin{bmatrix} K_F & (K_{cr})_i^T \\ (K_{cr})_i & 0 \end{bmatrix}\begin{Bmatrix} \varepsilon_{i+1} \\ (\lambda_{cr})_{i+1} \end{Bmatrix} = \begin{Bmatrix} R_i \\ (R_{cr})_i \end{Bmatrix} \tag{66}$$

Note again that the Jacobian and its transpose should be updated at each solution step.

2.7.3. Equations of motion with additional displacement constraints

For a general beam configuration that consists of both absolute and relative displacement constraints, one may define the total constraint-related matrices as

$$\lambda_c = \begin{Bmatrix} \lambda_{ca} \\ \lambda_{cr} \end{Bmatrix}, \quad K_c = \begin{Bmatrix} K_{ca} \\ K_{cr} \end{Bmatrix}, \quad R_c = \begin{Bmatrix} R_{ca} \\ R_{cr} \end{Bmatrix} \tag{67}$$

Therefore, the complete system equations of motion with the constraints can be given as a set of differential–algebraic equations.

$$\begin{bmatrix} M_F & 0 \\ 0 & 0 \end{bmatrix}\begin{Bmatrix} \ddot{\varepsilon} \\ \ddot{\lambda}_c \end{Bmatrix} + \begin{bmatrix} C_F & 0 \\ 0 & 0 \end{bmatrix}\begin{Bmatrix} \dot{\varepsilon} \\ \dot{\lambda}_c \end{Bmatrix} + \begin{bmatrix} K_F & K_c^T \\ K_c & 0 \end{bmatrix}\begin{Bmatrix} \varepsilon \\ \lambda_c \end{Bmatrix} = \begin{Bmatrix} R \\ R_c \end{Bmatrix} \tag{68}$$

2.8. Solution of the governing equations

In geometrically nonlinear static solutions, the time-dependent terms in Eq. (68) are omitted. In an iterative manner, the equations of motion becomes

$$\begin{Bmatrix} \varepsilon \\ \lambda_c \end{Bmatrix}_{k+1} = \begin{bmatrix} K_F & K_c^T \\ K_c & 0 \end{bmatrix}_k^{-1}\begin{Bmatrix} R \\ R_c \end{Bmatrix}_k \tag{69}$$

Note that K_F in the stiffness matrix is always constant, while K_c needs to be updated at each iteration. One problem associated with this approach is that it may lead to numerical instability when the beam is very flexible and large changes may happen to the right hand side from one solution to the next. With numerical damping added, the incremental form of the solution is

$$\begin{Bmatrix} \varepsilon \\ \lambda_c \end{Bmatrix}_{k+1} = \alpha_N\begin{Bmatrix} \varepsilon \\ \lambda_c \end{Bmatrix}_k + (1-\alpha_N)\begin{bmatrix} K_F & K_c^T \\ K_c & 0 \end{bmatrix}_k^{-1}\begin{Bmatrix} R \\ R_c \end{Bmatrix}_k \tag{70}$$

where α_N is the numerical damping parameter, ranging between 0 and 1. When $\alpha_N = 1$, the solution is stationary. When $\alpha_N = 0$, the solution is equivalent to Eq. (69).

Nonlinear transient solution of the beam is obtained by numerical integration of Eq. (68). As the formulation is developed for simulating nonlinear aeroelastic response of very flexible aircraft, the numerical integration scheme adopted should be able to provide easy solution for combined aeroelastic and flight dynamic degrees of freedom. In addition, the solution should be numerically stable in a long time scale, to facilitate the time simulation of aircraft flight. In view of the requirements, a modified first- and second-order Generalized-α Method along with an implicit subiteration scheme were developed by Shearer and Cesnik (2006), and it is applied to solve the governing equations in the current nonlinear strain-based formulation. Details about the integration scheme can be found in the reference.

3. Numerical studies

The strain-based nonlinear beam formulation is implemented in the numerical framework UM/NAST: The University of Michigan's Nonlinear Aeroelastic Simulation Toolbox. In the numerical studies, geometrically nonlinear static solutions and transient responses under forced dynamic excitations in UM/NAST are studied and compared to those from displacement-based MSC.Nastran (2003) and mixed-form UM/NLABS (Palacios and Cesnik, 2008).

3.1. Geometrically nonlinear static solution

Consider a slender cantilever isotropic beam whose geometric and physical properties are listed in Table 1. As shown in Fig. 6, a concentrated force is applied at the beam tip, with its axial component being zero, lateral component F_y^{pt} being 200 *N*, and vertical component F_z^{pt} being 30 *N*. The beam is solved in UM/NAST, MSC.Nastran, and UM/NLABS, respectively, with the beam discretization varied from 2 to 20 elements. CBEAM element is selected in the MSC.Nastran model. Note that if the beam is divided into n elements, the dimensions of the models are $4 \times n$ in the UM/NAST model, $6 \times n$ in the MSC.Nastran model, and $12 \times n$ in the UM/NLABS model, respectively. The lateral and vertical tip displacements obtained from the three solutions are plotted in Fig. 7 with the change of model dimensions. From the comparison, it is evident that to reach the same converged solution, the dimension of the strain-based model is smaller than the other two, especially the mixed-form model. Therefore, the strain-based formulation can capture the nonlinear beam deformation with fewer degrees of freedom. One may find another advantage of the strain-based formulation by looking into the solution procedures of the three solutions. The strain-based solution only needs a one-time inversion to the stiffness matrix, since this matrix is constant for the beam configuration. The others require updating the stiffness matrix iteratively due to the geometric stiffening effect when the beam is loaded. Therefore, the inversion operation to the stiffness matrix is required at each time when the stiffness matrix is updated. This advantage of the strain-based formulation makes it efficient in solving geometrically nonlinear static problems.

3.2. Transient response of split-beam

This section is to verify the kinematic formulation of split-beam systems. Fig. 8 exemplifies a split-beam system with two branches splitting from each other. The split-beam has the same cross-sectional properties as the single cantilever beam used previously. Each of the branches is discretized into 10 elements in both UM/

Table 1
Properties of the cantilever isotropic beam.

Mass per span (m)	0.10	kg/m
Span (L)	1.00	m
Rotational moment of inertia (I_{xx})	1.30×10^{-4}	kg m
Flat bending moment of inertia (I_{yy})	5.00×10^{-6}	kg m
Edge bending moment of inertia (I_{zz})	1.25×10^{-4}	kg m
Extensional rigidity ($k_{11} = EA$)	1.00×10^{6}	N
Torsional rigidity ($k_{22} = GJ$)	80.0	N m^2
Flat bending rigidity ($k_{33} = EI_y$)	50.0	N m^2
Edge bending rigidity ($k_{44} = EI_z$)	1.25×10^{3}	N m^2

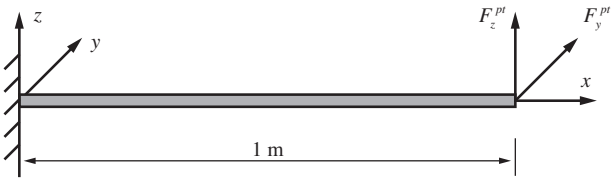

Fig. 6. Cantilever beam with tip loads.

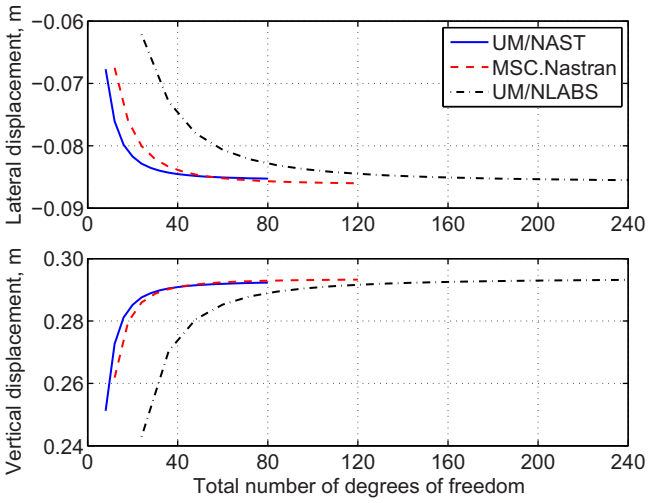

Fig. 7. Convergence of the static solutions in UM/NAST, MSC.Nastran, and UM/NLABS.

NAST and MSC.Nastran models. A sinusoidal vertical force is applied at the front tip, given by

$$F_z^{pt}(t) = \begin{cases} 0 & N \quad (t < 0) \\ A_F \sin \omega_F t & N \quad (t \geqslant 0) \end{cases} \tag{71}$$

with $A_F = 30\ N$ and $\omega_F = 20$ rad/s. The time responses of both tips are plotted in Fig. 9 and compared with the results from MSC.Nastran. The time steps used are 0.0025 s in UM/NAST and 0.002 s in MSC.Nastran to reach the converged results. The two sets of results are on top of each other.

3.3. Transient response of beam with relative displacement constraint

The Lagrange multiplier formulation for relative nodal displacement constraints is tested in this section. Beams with absolute nodal displacement constraints are not discussed here since they are generally not applicable to aircraft structures. For a joined-beam model, the two cantilever beam members meet at their tips. The cross-sectional properties of each beam member are still the same as defined before, with the geometry shown in Fig. 10. Each beam member is discretized into 20 elements in both UM/NAST and MSC.Nastran models.

To test the time simulation for the joined-beam model with the relative displacement constraint, a sinusoidal force governed by Eq. (71) is applied at the common tip of the two members in the vertical direction, with $A_F = 60\ N$ and $\omega_F = 20$ rad/s. Results from UM/

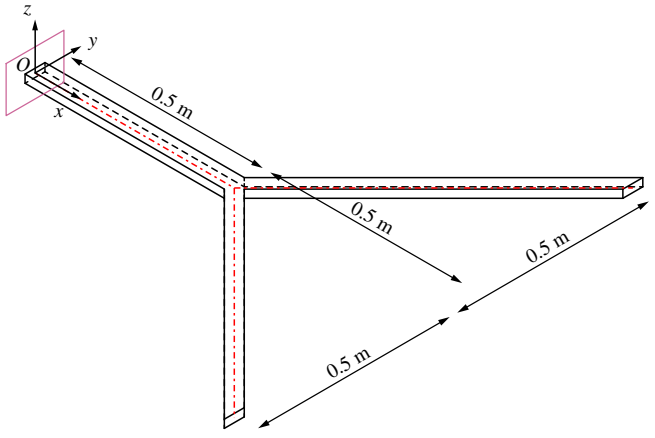

Fig. 8. Model description of a split-beam system.

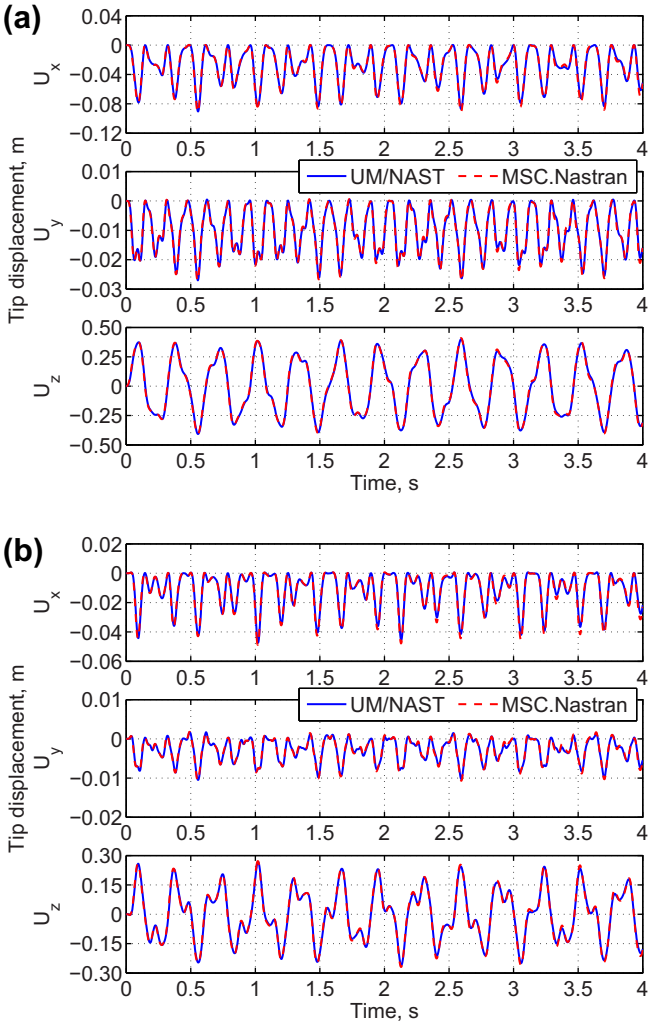

Fig. 9. Tip displacements the split-beam system under single tip load: (a) front tip; (b) rear tip.

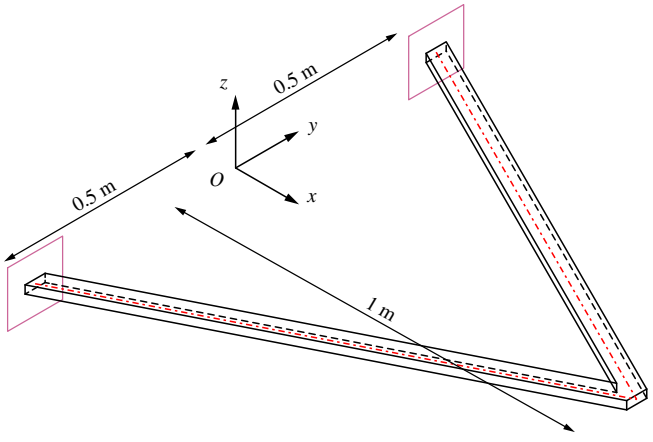

Fig. 10. Model description of a joined-beam system.

NAST and MSC.Nastran are compared in Fig. 11. The time steps used are 0.002 s in UM/NAST and 0.0016 s in MSC.Nastran. Good agreement between the two sets of results can be observed. In addition, the accuracy of the modeling of the relative nodal displacement constraints using the strain-based formulation may be

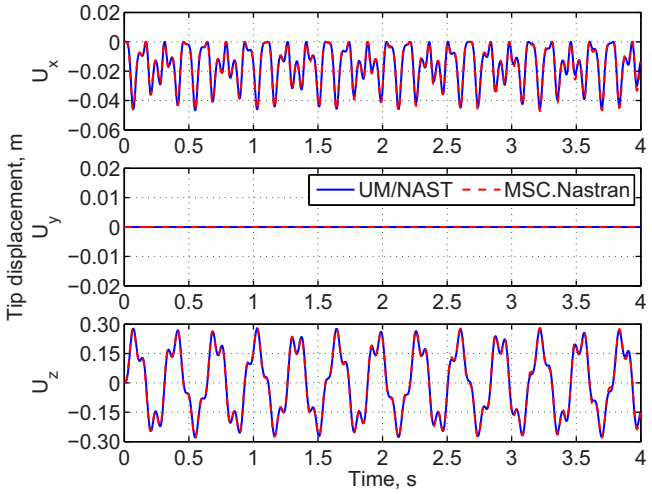

Fig. 11. Tip displacement of the joined-beam under vertical tip load.

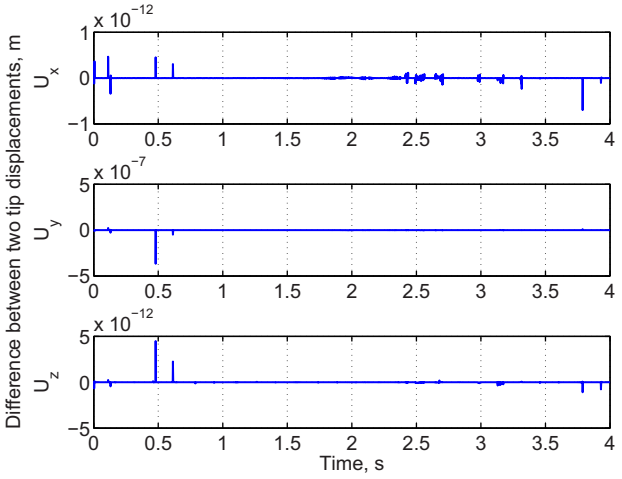

Fig. 12. Difference between the displacements of the two tips in the joined-beam under vertical tip load (results from UM/NAST).

examined by comparing the two beam tips' displacements from UM/NAST (Fig. 12). The displacements are almost identical, while demonstrating some numerical differences at a few time steps. The maximum difference between the two tip displacements is at the order of 10^{-7}, compared to the beam span. Therefore, the modeling of the nodal displacement constraint is correct.

3.4. Transient response of cantilever composite beam

Composite materials are widely used in aircraft structures. This section illustrates the capability of the strain-based formulation in solving composite beams. A slender composite beam is created with the geometric and physical properties listed in Table 2. The mixed-form solution from UM/NLABS (Palacios and Cesnik, 2008) is used for the comparison with that of UM/NAST. The wing is discretized into 20 elements in both UM/NAST and UM/NLABS models.

Table 2
Properties of the cantilever composite beam.

Mass per span (m)	0.185	kg/m	k_{11}	2.23×10^6	N
Span (L)	1.00	m	k_{12}	0	N m
I_{xx}	5.84×10^{-4}	kg m	k_{13}	-1.47×10^3	N m
I_{xy}	0	kg m	k_{14}	-5.24×10^4	N m
I_{xz}	0	kg m	k_{22}	63.2	N m^2
I_{yy}	1.05×10^{-5}	kg m	k_{23}	0	N m^2
I_{yz}	2.87×10^{-6}	kg m	k_{24}	0	N m^2
I_{zz}	5.74×10^{-4}	kg m	k_{33}	1.26×10^2	N m^2
r_y	-2.36×10^{-2}	m	k_{34}	34.7	N m^2
r_z	6.11×10^{-4}	m	k_{44}	6.92×10^3	N m^2

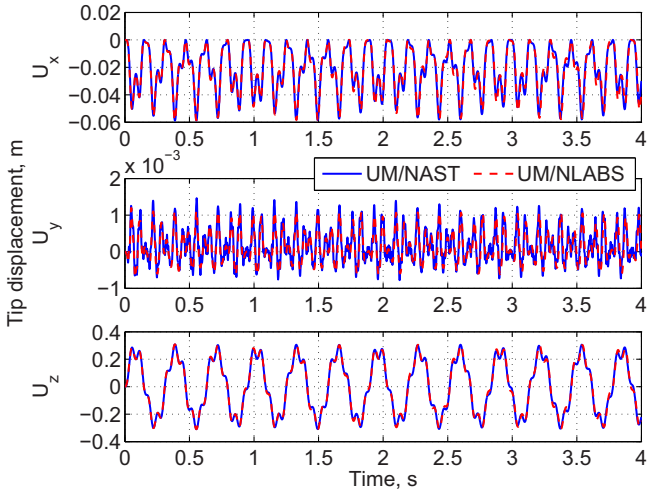

Fig. 13. Tip displacement of the cantilever composite beam under vertical tip load.

A sinusoidal point force governed by Eq. (71) is applied at the beam tip in the vertical direction, with $A_F = 100$ N and $\omega_F = 20$ rad/s. The root of the beam is fixed. The tip displacements of the beam are plotted in Fig. 13. The time steps used in UM/NAST and UM/NLABS are both 0.001 s. All results are showing good agreement. Note that the kinematics for split-beam systems and the Lagrange multiplier formulation for absolute and relative nodal displacement constraints are still applicable to composite beams. The strain-based formulation has been applied to the nonlinear aeroelastic analysis of very flexible aircraft with composite wings (Cesnik and Su, 2005).

4. Conclusions

A strain-based geometrically nonlinear beam formulation was presented, which is able to capture the arbitrarily large deformations of slender structures. With beam extension strain and bending/twist curvatures as independent degrees of freedom, the strain-based beam formulation makes no approximation to the deformation of beam reference line. Therefore, this formulation is geometrically exact and can accurately model the composite beam deformation. The strain-based formulation features fewer degrees of freedom than the displacement-based and the mix-form formulations to represent the same deformation complexity. In addition, this formulation solves directly for the beam curvatures that are the variables measured by typical sensors in control studies (e.g., strain gages). It also provides a constant generalized stiffness matrix, which greatly simplifies geometrically nonlinear static solutions. The strain-based beam formulation can effectively catch the geometrically nonlinear behavior of flexible isotropic and composite wings and provide the structural dynamic models for nonlinear aeroelastic and control studies of very flexible slender structures.

The beam equations of motion are derived through the principal of virtual work. Finite-element approach is used to solve the equations. To facilitate modeling of complete flexible aircraft, multiple-connected and statically indeterminate beam systems are considered. Kinematic relations of the strain-based formulation are

developed to model split-beam systems. Nodal displacement constraints are introduced through the Lagrange multiplier method. With the formulation for these complex beam configurations, arbitrary aircraft configurations can be modeled with the strain-based formulation.

The strain-based beam formulation, including the kinematics for split-beam systems, and the relative (inter-member) nodal displacement constraints, is compared to the displacement-based formulation (MSC.Nastran) and the mixed-form formulation (UM/NLABS). Results have shown that the strain-based formulation can capture the nonlinear beam behavior as what the displacement-based and the mixed-form formulations can do, with the advantages of requiring fewer degrees of freedom to model the arbitrary complex beam deformation. As one implementation of the strain-based beam formulation, UM/NAST (The University of Michigan's Nonlinear Aeroelastic Simulation Toolbox) has been successfully used for the coupled nonlinear aeroelastic, flight dynamic, and control studies of different very flexible aircraft.

Acknowledgments

This work was sponsored by AFOSR Grant F49620-02-1-0425, with Clark Allred (Capt., USAF) as the task technical monitor. The authors want to acknowledge Eric L. Brown (Draper Laboratory) for his contribution to the initial development of the strain-based beam formulation. Technical discussions with Christopher M. Shearer (Lt. Colonel, USAF) are gratefully acknowledged. Finally, the authors appreciate Devesh Kumar (University of Michigan) for providing the numerical results using the mixed-form beam formulation.

References

Bauchau, O.A., Hong, C.H., 1988. Nonlinear composite beam theory. Journal of Applied Mechanics – Transactions of the ASME 55 (1), 156–163.

Cesnik, C.E.S., Brown, E.L., 2002. Modeling of high aspect ratio active flexible wings for roll control. Paper No. AIAA-2002-1719. In: 43rd AIAA/ASME/ASCE/AHS/ASC Structures, Structural Dynamics, and Materials Conference, April 22–25, Denver, CO.

Cesnik, C.E.S., Brown, E.L., 2003. Active wing warping control of a joined-wing airplane configuration. Paper No. AIAA-2003-1715. In: 44th AIAA/ASME/ASCE/AHS/ASC Structures, Structural Dynamics, and Materials Conference, April 7–10, Norfolk, VA.

Cesnik, C.E.S., Hodges, D.H., 1997. VABS: a new concept for composite rotor blade cross-sectional modeling. Journal of the American Helicopter Society 42 (1), 27–38.

Cesnik, C.E.S., Su, W., 2005. Nonlinear aeroelastic modeling and analysis of fully flexible aircraft. Paper No. AIAA-2005-2169. In: 46th AIAA/ASME/ASCE/AHS/ASC Structures, Structural Dynamics, and Materials Conference, April 18–21, Austin, TX.

Gams, M., Planinc, I., Saje, M., 2007a. The strain-based beam finite elements in multibody dynamics. Journal of Sound and Vibration 305 (1–2), 194–210.

Gams, M., Saje, M., Srpčič, S., Planinc, I., 2007b. Finite element dynamic analysis of geometrically exact planar beams. Computers and Structures 85 (17–18), 1409–1419.

Hodges, D.H., 1990. A mixed variational formulation based on exact intrinsic equations for dynamics of moving beams. International Journal of Solids and Structures 26 (11), 1253–1273.

Hodges, D.H., 2003. Geometrically exact, intrinsic theory for dynamics of curved and twisted anisotropic beams. AIAA Journal 41 (6), 1131–1137.

Hodges, D.H., Shang, X., Cesnik, C.E.S., 1996. Finite element solution of nonlinear intrinsic equations for curved composite beams. Journal of the American Helicopter Society 41 (4), 313–321.

Livne, E., Weisshaar, T.A., 2003. Aeroelasticity of nonconventional airplane configurations – past and future. Journal of Aircraft 40 (6), 1047–1065.

MSC.Software, 2003. MSC.Nastran 2004 Quick reference Guide – Volume 1. MSC.Software Corporation, Santa Ana, CA.

Palacios, R., Cesnik, C.E.S., 2005. Cross-sectional analysis of nonhomogeneous anisotropic active slender structures. AIAA Journal 43 (12), 2624–2638.

Palacios, R., Cesnik, C.E.S., 2008. Geometrically nonlinear theory of composite beams with deformable cross sections. AIAA Journal 46 (2), 439–450.

Palacios, R., Cesnik, C.E.S., 2009. Structural models for flight dynamic analysis of very flexible aircraft. Paper No. AIAA-2009-2403. In: 50th AIAA/ASME/ASCE/AHS/ASC Structures, Structural Dynamics, and Materials Conference, May 4–7, Palm Springs, CA.

Patil, M.J., Hodges, D.H., Cesnik, C.E.S., 2000. Nonlinear aeroelastic analysis of complete aircraft in subsonic flow. Journal of Aircraft 37 (5), 753–760.

Patil, M.J., Hodges, D.H., Cesnik, C.E.S., 2001a. Limit-cycle oscillations in high-aspect-ratio wings. Journal of Fluids and Structures 15 (1), 107–132.

Patil, M.J., Hodges, D.H., Cesnik, C.E.S., 2001b. Nonlinear aeroelasticity and flight dynamics of high-altitude long-endurance aircraft. Journal of Aircraft 38 (1), 88–94.

Planinc, I., Saje, M., Čas, B., 2001. On the local stability condition in the planar beam finite element. Structural Engineering and Mechanics 12 (5), 507–526.

Ryu, H.-S., Sin, H.-C., 1996. Curved beam elements based on strain fields. Communications in Numerical Methods in Engineering 12 (11), 767–773.

Shang, X., Hodges, D.H., Peters, D.A., 1999. Aeroelastic stability of composite hingeless rotors in hover with finite-state unsteady aerodynamics. Journal of the American Helicopter Society 44 (3), 206–221.

Shearer, C.M., Cesnik, C.E.S., 2006. Modified generalized-α method for integrating governing equations of very flexible aircraft. Paper No. AIAA-2006-1747. In: 47th AIAA/ASME/ASCE/AHS/ASC Structures, Structural Dynamics, and Materials Conference, May 1–4, Newport, RI.

Shearer, C.M., Cesnik, C.E.S., 2007. Nonlinear flight dynamics of very flexible aircraft. Journal of Aircraft 44 (5), 1528–1545.

Su, W., Cesnik, C.E.S., 2010. Nonlinear aeroelasticity of a very flexible blended-wing-body aircraft. Journal of Aircraft 47 (5), 1539–1553.

Tilmann, C.P., Flick, P.M., Martin, C.A., Love, M.H., 2003. High-altitude long endurance technologies for sensorcraft. Paper No. MP-104-P-26. In: RTO AVT-099 Symposium on Novel and Emerging Vehicle and Vehicle Technology Concepts, April 7–11, Brussels, Belgium.

Zienkiewicz, O.C., Taylor, R.L., 2000. The finite element method, . The Basis, Fifth ed., vol. 1. Butterworth-Heinemann, Woburn, MA.

Zupan, D., Saje, M., 2003. Finite-element formulation of geometrically exact three-dimensional beam theories based on interpolation of strain measures. Computer Methods in Applied Mechanics and Engineering 192 (49–50), 5209–5248.